2D/2D Heterojunction Interfaces of 1T-MoS_2 and Ti_3C_2 MXene: Designing High-Performance Catalyst for the Hydrogen Evolution Reaction

Sana Akir[1], Bastian Schmiedecke[1], Debabrata Bagchi[2], Jan Plutnar[3], Prashanth W. Menezes[2,4], Yael Rodriguez-Ayllon[5,6], Yan Lu[5,6], Zdenek Sofer[3], and Michelle P. Browne[1]*

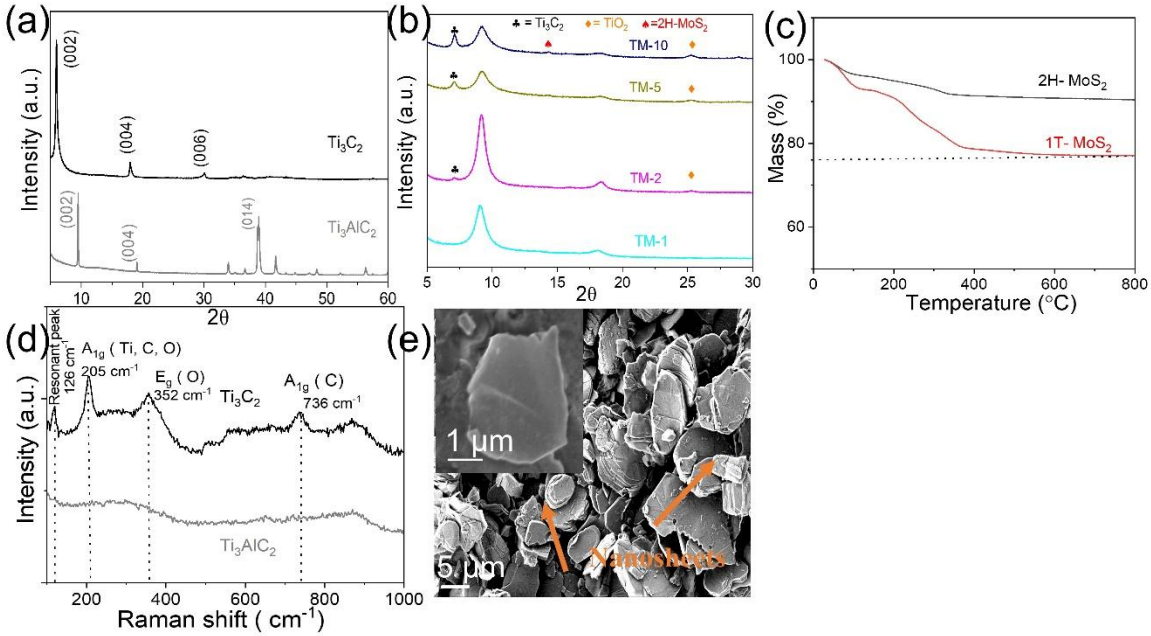

Figure S1. (a) XRD of Ti_3C_2 and Ti_3AlC_2, (b) zoomed-in XRD of composites from 5 to 30°, (c) TGA curves of 2H-MoS_2 and 1T-MoS_2, (d) XRD of Ti_3C_2 and Ti_3AlC_2, and (e) SEM of delaminated Ti_3C_2 MXene.

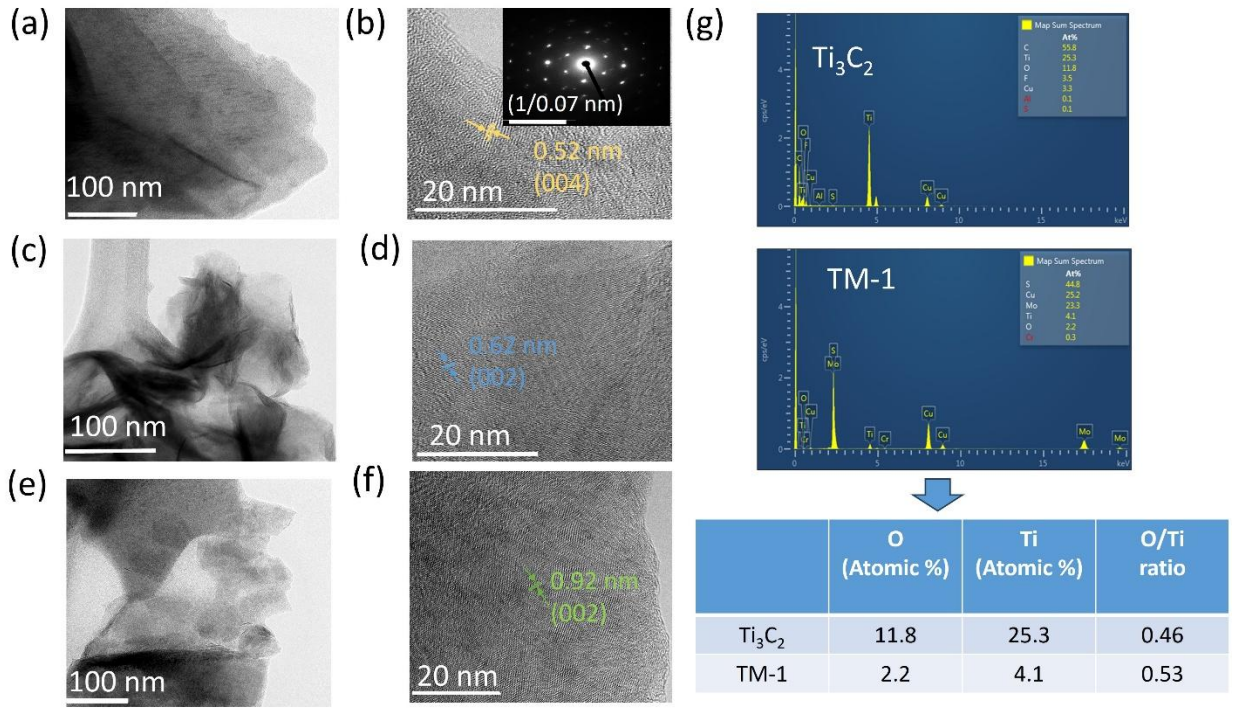

	O (Atomic %)	Ti (Atomic %)	O/Ti ratio
Ti_3C_2	11.8	25.3	0.46
TM-1	2.2	4.1	0.53

Figure S2. (a) TEM of Ti_3C_2, (b) HRTEM of Ti_3C_2 (Inset: SAED of Ti_3C_2), (c, d) TEM and HRTEM of 2H-MoS_2, (e, f) TEM and HRTEM of 1T-MoS_2, (g) EDS spectra of Ti_3C_2 and TM-1 and their corresponding O/Ti atomic % ratio

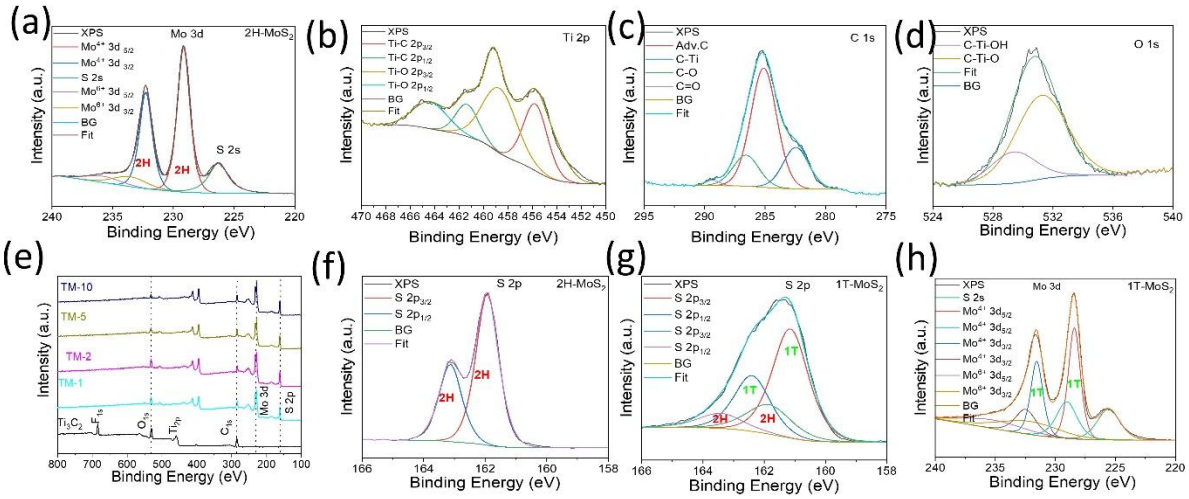

Figure S3. (a) XPS survey spectra of Ti_3C_2 and composites, high-resolution XPS spectra of Ti_3C_2: (b) Ti 2p, (c) C 1s, and (d) O1s, High-resolution XPS spectra of Mo 3d in: (e) 2H-MoS_2, and (f) 1T-MoS_2, High-resolution XPS spectra of S 2p in: (g) 2H-MoS_2, and (h) 1T-MoS_2

Table S1a. Report the full-width-half-maximum (FWHM) values for the XPS deconvoluted peaks of Mo 3d

Sample	**1T $3d_{5/2}$**	**1T $3d_{3/2}$**	**2H $3d_{5/2}$**	**2H $3d_{3/2}$**	**Mo (VI) $3d_{5/2}$**	**Mo (VI) $3d_{3/2}$**	**S 2s**
TM-1	1.28	1.28	1.83	1.83	5.35	5.35	2.68
TM-2	1.24	1.24	2.00	2.00	3.60	3.60	2.52
TM-5	1.24	1.24	1.91	1.91	4.42	4.42	2.50
TM-10	1.22	1.22	2.18	2.18	3.80	3.80	2.51

The 5/2 and 3/2 components of the same type of electrons are constrained, meaning their FWHMs are forced to be equal. The lower FWHMs of the 1T phase correspond to its conducting, metallic behavior, confirming the assignment of the 1T/2H phase.

These values fall within expected ranges for chemically distinct Mo species in MoS_2-based materials. The narrower FWHMs of the 1T-MoS_2 components (~1.22-1.28 eV) relative to those of the 2H-MoS_2 peaks (~1.83-2.18 eV) are consistent with the more delocalized electronic structure of the 1T phase, which arises from its metallic, octahedrally coordinated Mo environment. In contrast, the broader 2H peaks reflect its semiconducting character and the increased chemical disorder associated with 2H domains in the mixed-phase composite. Furthermore, the significantly broader FWHMs for the Mo (VI) peaks (3.6-5.35 eV) likely reflect the contribution from multiple surface oxidation species.

Table S1b. Deconvoluted peak areas of the S 2p region from XPS analysis and calculated 1T phase content of MoS_2.

Sample	1T $S2p_{3/2}$	1T $S2p_{1/2}$	2H $S2p_{3/2}$	2H $S2p_{1/2}$	% 1T-MoS_2
TM-1	31495.5	16094.2	4132.1	2111.5	89
TM-2	25484.5	13022.6	3701.8	1891.6	87
TM-5	16942.8	8657.8	3191.0	1630.6	84
TM-10	26902.2	13747.0	5163.4	2638.5	83

The percentage of 1T-MoS_2 was determined by integrating the areas of the deconvoluted S $2p_{3/2}$ and S $2p_{1/2}$ peaks corresponding to both the 1T and 2H phases of MoS_2. The 1T phase content was calculated using the following formula:

$$1T\text{-}MoS_2\ (\%) = (A_{1T} / (A_{2H} + A_{1T})) \times 100$$

where A_{1T} and A_{2H} represent the total integrated areas of the S 2p peaks attributed to the 1T and 2H phases, respectively.

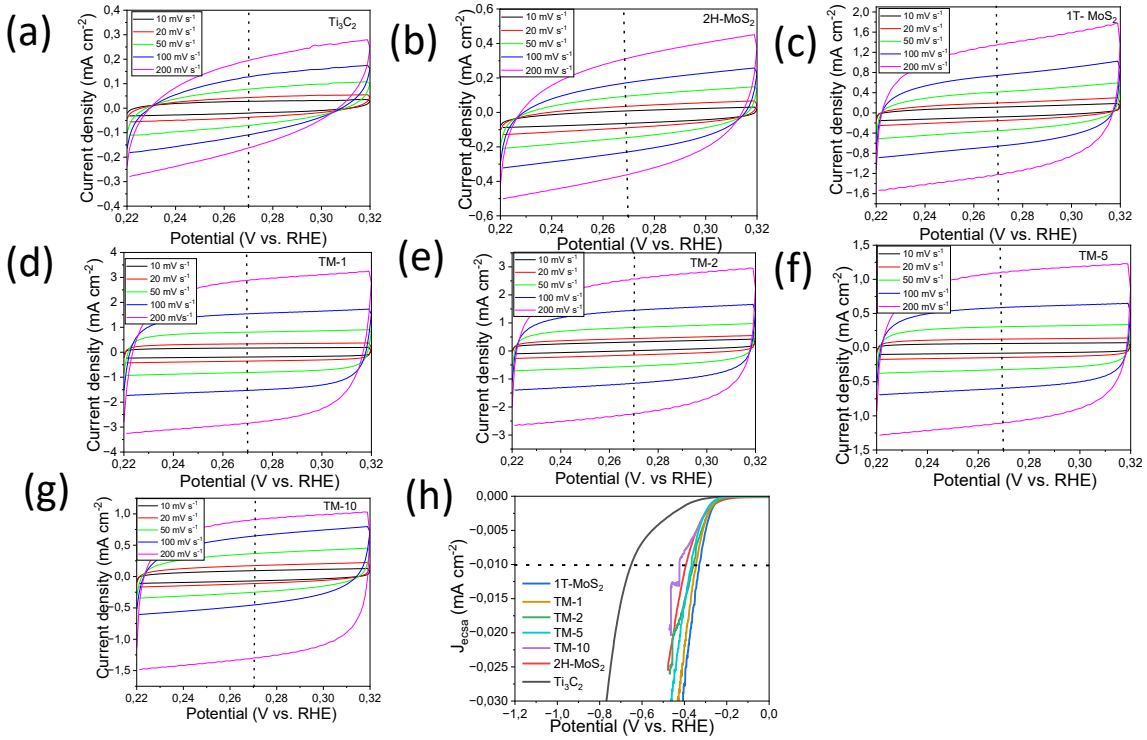

Figure S4. Cyclic voltammograms obtained from the non-faradic region of: (a) Ti_3C_2, (b) 2H-MoS_2, (c) 1T-MoS_2, (d) TM-1, (e) TM-2, (f) TM-5, (g) TM-10 at different scan rates in 0.5M H_2SO_4, and (h) ECSA normalized LSV of all catalysts

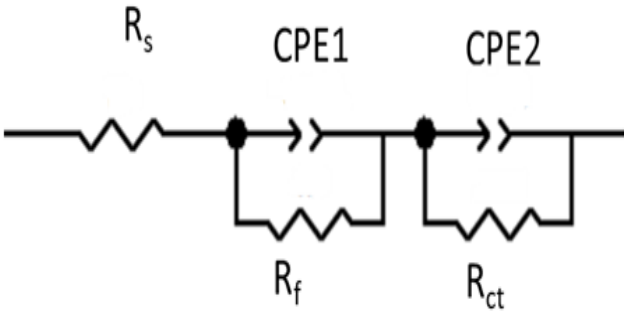

Figure S5. Equivalent circuit used to stimulate the Nyquist plot where: Rs: solution resistance, R_f and CPE_1 are related to the porosity of the electrode; R_{ct}: charge transfer resistance, CPE_2 is

related to the interface between catalyst and electrolyte; CPE represents constant phase element.

(EIS data fitted by ZView software)

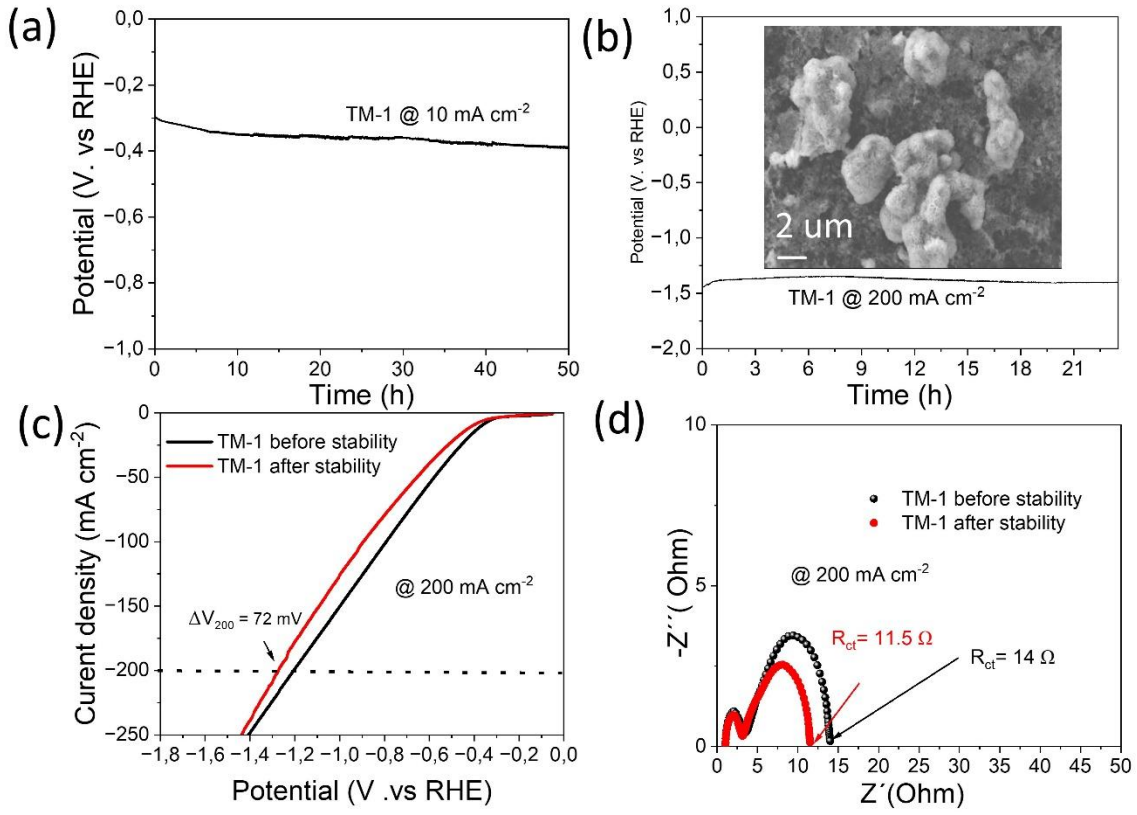

Figure S6. (a) Stability test of TM-1 under constant current density of 10 mA cm^{-2} for 50 h, (b) Stability test of TM-1 under constant current density of 200 mA cm^{-2} for 24 h (inset: SEM of TM-1 after stability test), (c) LSV, and (d) EIS of TM-1 before and after stability test under J= 200 mA cm^{-2}

Table S2. Comparison of the electrocatalytic performance of Ti_3C_2/1T-MoS_2 with (1T, 2H) MoS_2 and other MoS_2-MXene-based materials for the hydrogen evolution reaction (HER).

Catalysts	Overpotential η_{10} [mV]	Tafel Slope [mV·dec^{-1}]	Mass loading	Synthesis method	Electrolyte	References
Ti_3C_2/ 1T-MoS_2	248	55	0.32 mg cm^{-2}	Hydrothermal	0.5 M H_2SO_4	This work
Ti_3C_2/ MoS_2 (1T-2H)	280	83.8	0.44 mg cm^{-2}	Hydrothermal+ Interfacial Assembly	0.5 M H_2SO_4	[1]
MoS_2/Ti_3C_2	400	68	0.35	hydrothermal method	0.5 M H_2SO_4	[2]
TCO/MoS_2	269	82	3.8	One-pot solvothermal synthesis	0.5 M H_2SO_4	[3]
MoS_2 QDs/$Ti_3C_2T_x$	220	72	0.354	Electrostatic self-assembly	0.5 M H_2SO_4	[4]
MoS_2-MXene	307	68.5	-	hydrothermal method	0.5 M H_2SO_4	[5]
$Ti_3CN(OH)_x$@MoS_2	120	64	0.408	Hydrothermal method	0.5 M H_2SO_4	[6]
$Mo_2Ti_2C_3T_x$/MoS_2	298	112	0.2	microwave-assisted hydrothermal method	1 M KOH	[7]
MoS_2/Ti_3C_2 MXene	421	217	-	Hydrothermal method	1 M NaOH	[8]
MoS_2/Nb_2CT_x	127	56.3	-	hydrothermal method	0.5 M H_2SO_4	[9]
MoS_2-$Ti_3C_2T_x$	152	70	0.28	combining liquid nitrogen-freezing and subsequent annealing.	0.5 M H_2SO_4	[10]
MoS_2-Nb_2CT_x	141	93.4	-	hydrothermal method	1 M KOH	[9]
Fe_2O_3/MoS_2/$Ti_3C_2T_x$ MXene	123	71	-	hydrothermal synthesis	0.5 M H_2SO_4	[11]

2H-MoS_2	369	137	0.26 ug.cm^{-2}	solid-state reaction and annealing	0.5 M H_2SO_4	[12]
2H-MoS_2 1T-2H MoS_2	342 212	78 131	-	CVD	0.5 M H_2SO_4	[13]
1T-MoS_2	230	58.47	0.46 mg cm^{-2}	Solvothermal	0.5 M H_2SO_4	[14]
1T-MoS_2	235	106	1 mg cm^{-2}	Hydrothermal	0.5 M H_2SO_4	[15]
1T/2H MoS_2	255	44	0.285 mg cm^{-2}	Hydrothermal	0.5 M H_2SO_4	[16]
p-MoS2	260	53.6	0.285 mg cm^{-2}	micro-reaction	0.5 M H_2SO_4	[17]
1T-MoS_2	292	55.7	0.28 mg cm^{-2}	Hydrothermal	0.5 M H_2SO_4	[18]

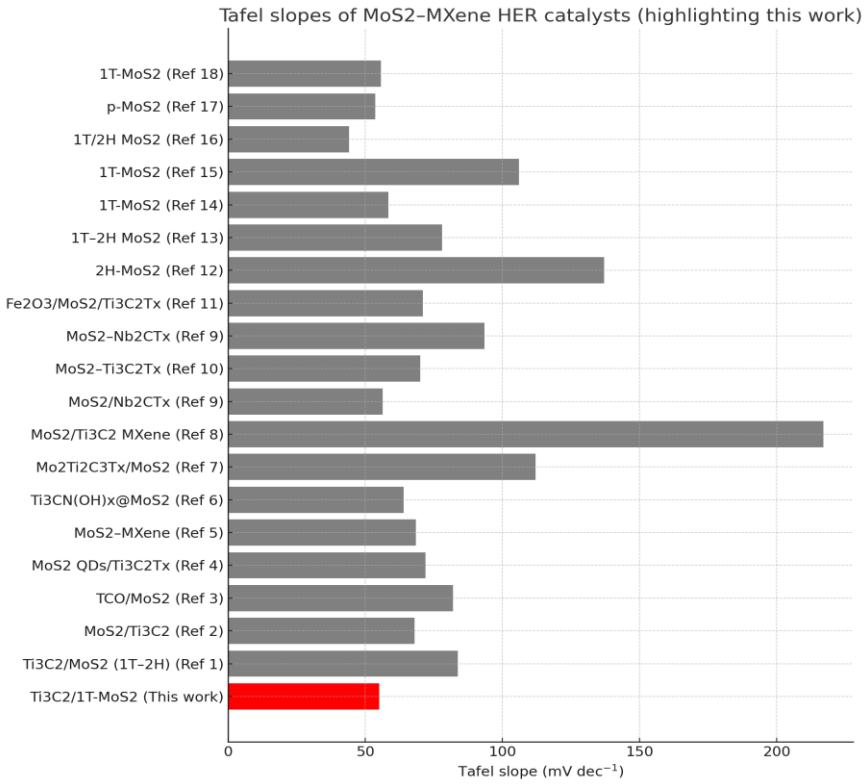

Figure S7. Bar chart comparing the Tafel slopes of MoS_2-MXene-based HER catalysts. The Ti_3C_2/1T-MoS_2 catalyst from this work is highlighted in red. Reference numbers correspond to those listed in Table S2.

Table S3 EIS fitting parameters from the equivalent circuit for different samples

Samples	**R_S (Ω)**	**R_f (Ω)**	**CPE_1 (S s^{-n})**	**R_{ct} (Ω)**	**CPE_2 (S s^{-n})**
1T-MoS_2	1.3	15.9	9.18E-7	133	3.69E-3
TM-1	1	9.3	9.360E-7	91	9.070E-3
TM-2	1.1	20.1	5.71E-7	181	4.356E-4
TM-5	1.2	22.4	4.08E-7	238	6.009E-4
TM-10	1.4	28.6	1.831E-7	428	2.79E-4

Table S 4. The estimated $C_{dl,}$ and the corresponding ECSA of different samples

Catalysts	C_{dl} (mF cm^{-2})	ECSA (cm^2)
TM-1	14	350
TM-2	11.8	295
TM-5	5.45	136.25
TM-10	4.5	112.5
1T-MoS_2	6.16	154
2H-MoS_2	1.82	45.5
Ti_3C_2	0.8	20

References

1. Loh JY, Yap FM, Ong W-J. 2D/2D heterojunction interface: Engineering of 1T/2H MoS2 coupled with Ti3C2Tx heterostructured electrocatalysts for pH-universal hydrogen evolution. *Journal of Materials Science & Technology* **179**, 86-97 (2024).

2. Huang L, Ai L, Wang M, Jiang J, Wang S. Hierarchical MoS2 nanosheets integrated Ti3C2 MXenes for electrocatalytic hydrogen evolution. *International Journal of Hydrogen Energy* **44**, 965-976 (2019).

3. Lontio Fomekong R*, et al.* Enhancing the Electrocatalytic Properties of a One-Pot Synthesis of Defect-Rich 2D/2D Nanoheterointerface of Titanium Carbo-Oxide and Molybdenum Disulfide for Hydrogen Evolution Reaction in Acidic Medium. *ACS Sustainable Chemistry & Engineering* **11**, 14528-14537 (2023).

4. Chen L*, et al.* Quasi zero-dimensional MoS2 quantum dots decorated 2D Ti3C2Tx MXene as advanced electrocatalysts for hydrogen evolution reaction. *International Journal of Hydrogen Energy* **47**, 10583-10593 (2022).

5. Raj SK, Sharma V, Mishra S, Kulshrestha V. MoS 2 quantum dot-modified MXene nanoflowers for efficient electrocatalytic hydrogen evolution reaction. *RSC Applied Interfaces* **1**, 1057-1068 (2024).

6. Jiang J*, et al.* Carbonitride MXene Ti3CN(OH)x@MoS2 hybrids as efficient electrocatalyst for enhanced hydrogen evolution. *Nano Research* **16**, 4656-4663 (2023).

7. Hanan A, Numan A, Norhaffis Mustafa M, Walvekar R, Khalid M. High-performance Mo2Ti2C3Tx/MoS2 hybrid electrocatalyst for sustainable hydrogen production. *International Journal of Hydrogen Energy* **161**, 150533 (2025).

8. Hasanah R*, et al.* Two-dimension MoS2/Ti3C2 MXene nanocomposite for an efficient hydrogen evolution reaction in alkaline media. *Materials Research Bulletin* **190**, 113514 (2025).

9. Hu L, Sun Y, Gong S-J, Zong H, Yu K, Zhu Z. Experimental and theoretical investigation on MoS2/MXene heterostructure as an efficient electrocatalyst for hydrogen evolution in both acidic and alkaline media. *New Journal of Chemistry* **44**, 7902-7911 (2020).

10. Liu J*, et al.* Hierarchical “nanoroll” like MoS2/Ti3C2Tx hybrid with high electrocatalytic hydrogen evolution activity. *Applied Catalysis B: Environmental* **241**, 89-94 (2019).

11. Dongre S S, Iqbal A, Thapa R, M P, Ramu S, Balakrishna RG. Synergistic Catalyst Design for Enhanced Electrochemical Hydrogen Evolution: Fe2O3/MoS2/Ti3C2Tx MXene Ternary Composite. *ACS Applied Engineering Materials* **2**, 943-954 (2024).

12. Guo X*, et al.* Charge self-regulation in 1T'''-MoS2 structure with rich S vacancies for enhanced hydrogen evolution activity. *Nature communications* **13**, 5954 (2022).

13. Hong Z, Hong W, Wang B, Cai Q, He X, Liu W. Stable 1T –2H MoS2 heterostructures for efficient electrocatalytic hydrogen evolution. *Chemical Engineering Journal* **460**, 141858 (2023).

14. Wang S*, et al.* One-Step Synthesis of 1T MoS2 Hierarchical Nanospheres for Electrocatalytic Hydrogen Evolution. *ACS Applied Energy Materials* **5**, 11705-11712 (2022).

15. Li Z*, et al.* Manipulating Coordination Structures of Mixed-Valence Copper Single Atoms on 1T-MoS2 for Efficient Hydrogen Evolution. *ACS Catalysis* **12**, 7687-7695 (2022).

16. Li H*, et al.* Controllable fabrication and structure evolution of hierarchical 1T-MoS2 nanospheres for efficient hydrogen evolution. *Green Energy & Environment* **7**, 314-323 (2022).

17. Shao M, Wang P, Wang Y, Wang B, Wang Y, Xu J. Continuous synthesis of few-layer MoS2 with highly electrocatalytic hydrogen evolution. *Green Energy & Environment* **6**, 858-865 (2021).

18. Rong J*, et al.* Restructuring electronic structure via W doped 1T MoS2 for enhancing hydrogen evolution reaction. *Applied Surface Science* **579**, 152216 (2022).